Author Manuscript

Author Manuscript

Author Manuscript

Author Manuscript

HHS Public Access

Author manuscript

ACS Infect Dis. Author manuscript; available in PMC 2023 March 23.

Published in final edited form as:

ACS Infect Dis. 2020 October 09; 6(10): 2592–2603. doi:10.1021/acsinfecdis.0c00156.

Structural basis for the regulation of biofilm formation and iron uptake in *A. baumannii* by the blue-light using photoreceptor, BlsA

Iva Chitrakar[1,2], **James N. Iuliano**[3], **YongLe He**[3], **Helena A. Woroniecka**[3], **Jinnette Tolentino Collado**[3], **Jinelle Wint**[1], **Stephen G. Walker**[4], **Peter J. Tonge**[2,3], **Jarrod B. French**[1,2,3,5,*]

[1]Department of Biochemistry and Cell Biology, Stony Brook University, Stony Brook, NY, USA, 11790

[2]Biochemistry and Structural Biology Program, Stony Brook University, Stony Brook, NY, USA, 11790

[3]Department of Chemistry, Stony Brook University, Stony Brook, NY, USA, 11790

[4]Department of Oral Biology and Pathology, Stony Brook University, Stony Brook, NY, USA, 11790

[5]The Hormel Institute, University of Minnesota, Austin, MN, 55912

Abstract

The opportunistic human pathogen, *A. baumannii*, senses and responds to light using the blue light sensing A (BlsA) photoreceptor protein. BlsA is a Blue Light Using FAD (BLUF) that is known to regulate a wide variety of cellular functions through interactions with different binding partners. Using immunoprecipitation of tagged BlsA in *A. baumannii* lysates, we observed a number of proteins that interact with BlsA, including several transcription factors. In addition to a known binding partner, the iron uptake regulator Fur, we identified the biofilm response regulator BfmR as a putative BlsA binding partner. Using microscale thermophoresis, we determined that both BfmR and Fur bind to BlsA with nanomolar binding constants. To better understand how BlsA interacts with and regulates these transcription factors, we solved the X-ray crystal structures of BlsA in both a ground (dark) state and a photo-activated light state. Comparison of the light- and dark-state structures revealed that, upon photoactivation, the two α-helices comprising the variable domain of BlsA undergo a distinct conformational change. The flavin binding site, however, remains largely unchanged from dark to light. These structures, along with docking studies of BlsA and Fur, reveal key mechanistic details about how BlsA propagates the photoactivation signal between protein domains and on to its binding partner. Taken together, our structural and biophysical data provide important insights into how BlsA controls signal transduction in *A. baumannii* and provides a likely mechanism for blue-light dependent modulation of biofilm formation and iron uptake.

Graphical Abstract

*To whom correspondence should be addressed: Jarrod B. French: jfrench@umn.edu; (507)437-9637.

Author Manuscript Author Manuscript Author Manuscript Author Manuscript

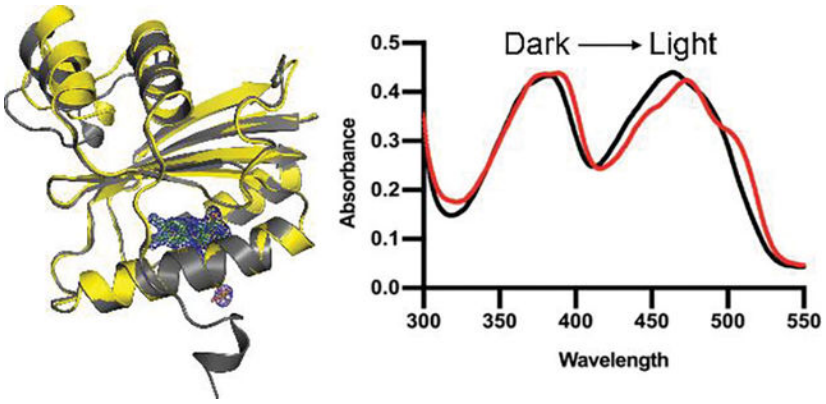

Keywords

BLUF; LOV; photoreceptor; biofilms; BfmR; FUR

The opportunistic pathogen, *Acinetobacter baumannii*, causes nosocomial infections that can be difficult to treat, in part because of the capacity of this bacterium to form biofilms on abiotic surfaces [1, 2]. Several studies have shown that a number of this organisms' physiological functions are regulated by light [3–5]. In response to blue light, *A. baumannii* modulates an array of pathways and gene clusters including those involved in cell motility, expression of efflux pumps for antibiotic resistance, and biofilm formation, among other functions [3, 6]. It's ability to respond to light is controlled by a Blue Light Using FAD (BLUF) photoreceptor called BlsA (blue-light-sensing A) [6, 7]. As with other BLUF domains, blue light induces the protein to change into a photoactivated signaling state. This signal is then transmitted through the protein to its respective effector domain, which is responsible for the resulting physiological output. BlsA is an example of a short BLUF, where the effector domain is a separate protein. This is in contrast to multi-domain BLUF like *Oscillaroria acuminata* (OaPAC), which has the BLUF and effector domains on the same polypeptide [8–11].

The effector domain that associates with the individual BLUF proteins dictates the downstream biological response. These domains vary widely, and can elicit their downstream effects *via* enzyme activity, protein-protein interactions or by acting as transcription factors [3, 9, 12–15]. For most known BLUF proteins, including AppA, OaPAC and PixD (a short BLUF from *Synechocystis sp.*) [14, 16, 17], there is a unique effector domain or binding partner that leads to the specific biological output. Photoactivation of BlsA leads to changes in expression levels for a wide range of proteins, including entire metabolic pathways [3, 6, 18]. This suggests that, unlike other BLUF proteins, BlsA may have multiple binding partners. To date, the only known binding partner of BlsA is the iron uptake regulator Fur [18]. The proposed interaction between BlsA and Fur helps to regulate iron homeostasis in a temperature-dependent fashion [7, 18, 19].

The complete photocycle of BLUF proteins involves the initial, ultrafast, photoexcitation of the chromophore, followed by slower, larger-scale conformational changes of the BLUF protein that lead to altered affinity for the effector domain. While there have been significant

Author Manuscript Author Manuscript Author Manuscript Author Manuscript

efforts to understand the photoactivation and signal transduction mechanisms in BLUF proteins, particularly using AppA and its binding partner PpsR, numerous questions still remain [9, 11]. BLUF domains undergo a characteristic ~10 nm redshift in the absorption spectrum upon photoexcitation, a direct indication of bonding changes around the non-covalently bound flavin chromophore. While still an active topic of research, there is a general consensus that the rotation or keto-enol tautomerization of a conserved glutamine side chain, is a key structural change that drives signal transduction [20–23]. A flavin radical may be an important reaction intermediate in the molecular mechanism in some cases [22, 24–26]. The tautomerization of the conserved glutamine leads to additional subtle rearrangements of the chromophore and the residues that directly interact with it. The signal transduction mechanisms that describe how this signal is propagated through the protein and on to the effector protein or domain, are still not well understood and may vary for each BLUF-effector pair.

In this study, we set out to define key features of the signal transduction mechanisms of BlsA and how these are exploited to regulate biofilm formation and other functions of *A. baumannii*. Using co-immuniprecipation with BlsA, we identified a novel binding partner, the transcription factor and biofilm response regulator BfmR, and quantified its interaction with BlsA. We then solved X-ray crystal structures of the ground state and a photo-activated state of BlsA. Upon photoactivation, BlsA undergoes a significant conformational change in the C-terminal pair of α-helices comprising the variable domain. From our data we propose a likely mechanism for intra-protein signal transduction. In addition, aided by protein-protein docking studies, we describe a putative mechanism for the light-induced regulation of BlsA interactions with its binding partners. This data provides important new insights into the physicochemical changes that occur in BlsA in response to light, and how these changes may contribute to the regulation of biofilm formation in *A. baumannii*.

RESULTS AND DISCUSSION

BlsA and its binding partners:

The short BLUF protein of BlsA senses and responds to blue light. Photoactivation of the flavin chromophore initiates a series of molecular events that ultimately leads to a distinct, physiologically relevant, output. After initial photoactivation, physicochemical changes in BlsA alter its affinity to an effector protein, which is ultimately responsible for the downstream biological output. To better understand the molecular mechanisms that underlie this process we first set out to identify potential binding partners of BlsA. To this end, we employed co-immunopreciptation to pull-down binding partners, followed by mass spectrometry for identification (Figure S1). N-terminally hexahistidine-tagged BlsA was treated with a heterobifunctional cross-linking reagent and then added to *A. baumannii* lysate. After a period of incubation, BlsA and its binding partners were covalently linked using the UV-induced cross-linking agent. The BlsA-protein complexes were isolated by immunoprecipitation on agarose beads, and extensively washed. The samples were then trypsin digested and identified using mass spectrometry. Note that it is possible that the UV light used to activate the cross-linking reagents may have induced a photoactive state in BlsA and, as such, the samples kept in the dark may not represent a true dark-state.

Author Manuscript Author Manuscript Author Manuscript Author Manuscript

Despite this limitation, the purpose of this experiment was to identify any BlsA binding partners for further characterization, and we expect that this approach would be sufficient to capture potential BlsA-binding partners. As expected, a number of proteins were identified, including metabolic proteins, membrane associated proteins and transcription factors (Table S1). As *A baumannii* is known to regulate a wide variety of genes in response to light [3], we decided to focus our investigations on transcription factors.

Amongst the transcription factors identified were several that could provide clues to how *A. baumannii* responds to light (Figure 1). Three of these, including ompR, AraC-type DNA-binding domain, and GH3 promoter, only appeared in samples exposed to light. OmpR plays a central role in osmotic stress response, while AraC-like regulators are known to control the expression of virulence factors in response to a wide variety of environmental stimuli [27–30]. The organism may benefit from coordinating these responses with photosensitivity, through the function of the photoreceptor BlsA. Of the handful of transcription factors that we definitively identified, the two most abundant proteins that co-precipitated with BlsA were the iron uptake regulator, Fur, and the biofilm response regulator, BfmR. These two proteins were also the only transcription factors that were observed in all samples that we tested, regardless of whether they were conducted with or without cross linkers under light or dark conditions. Fur has been previously identified as a BlsA binding partner using a yeast 2-hybrid screen [18]. BfmR is a response regulator of a two-component signal transduction system and acts as a transcriptional regulator [31, 32]. This transcription factor is a master regulator of biofilm formation, contributes to antibiotic resistance, and is essential for the survival of *A. baumannii* [32–35]. Notably, the N-terminal region of BfmR has a relatively high sequence similarity (27% sequence identity over 51% of the sequence) to the PixD binding partner and response regulator, PixE, which is involved in controlling chemotaxis. The identification of BfmR as a putative BlsA binding partner points to a likely mechanism for how light influences biofilm formation. Overall, these results also suggest that BlsA may indeed interact with multiple different effector proteins.

BlsA binding affinity to BfmR and Fur.

As a means to validate our results from the immunoprecipitation experiment we wished to independently confirm, *in vitro*, that BlsA physically interacts with its binding partners. We expressed and purified BlsA, BfmR and Fur proteins and quantified the binding affinity of these proteins using microscale thermophoresis (MST). While our initial data suggested that BlsA had a high affinity for BfmR, the BlsA protein sample was prone to aggregation over time and, thus, yielded relatively noisy data (Figure S2). To improve the protein stability, we expressed and purified a thioredoxin fusion of BlsA, TRX-BlsA. This variant was significantly more stable and behaved well under the conditions tested. For the MST experiments, we labeled TRX-BlsA with Alexa-Fluor 647 and used unlabeled BfmR and Fur. We observed tight binding of TRX-BlsA to both BfmR (Figure 2A) and Fur (Figure 2B) with calculated binding constants of 10 nM and 3.2 nM, respectively. Control experiments using BSA or TRX showed no significant binding to any of BlsA, BfmR or Fur (Figure 2C and FigureS3). As a further test of specificity, we measured the binding of an alternate BLUF domain protein, PixD [14, 36], to BfmR (Figure S3). As expected, we saw only very low, not physiologically relevant, binding affinity. Note that while these experiments

Author Manuscript Author Manuscript Author Manuscript Author Manuscript

were carried out in ambient light, the nature of the experimental setup kept the samples in the dark throughout the experiment. As such, we expect that these results represent predominantly ground sate interactions. The interactions *in vivo* could display a higher affinity than reported here, but would also be dependent on other local effects that could mediate the interactions such as the presence of other binding partners or crowding effects from the local cellular environment.

While the limitations of the MST instrument preclude the accurate measurement of binding affinities of the photo-activated form of BlsA, we instead conducted a series of on-column interaction experiments to confirm that the interaction between BlsA and its binding partners was light-dependent. We incubated hexahistidine-tagged BlsA with untagged FUR or untagged BfmR under dark or light conditions. After a 30-minute incubation time, we added these samples to Ni-NTA resin to bind the tagged BlsA. We then separated the unbound proteins (flowthrough) from the resin, and eluted bound proteins (elution) using 300 mM imidazole. The results (Figure 3) indicate that both FUR and BfmR bind more tightly to BlsA under dark conditions. Very little of either protein is seen bound to BlsA when the sample was illuminated. While this method does not provide a means to accurate measure binding affinities, we analyzed the ratio of the intensity of BlsA bands to binding partner bands and compared these ratios in flowthrough and elution fractions to approximate the relative binding affinity in light vs. dark (Figure S5). For BlsA:FUR, there was approximately 2--fold more protein bound to BlsA in the dark state, while for BlsA:BfmR, more than a 5-fold increase in the amount of protein was bound to BlsA in the dark state. While it is likely that other factors contribute to the strength of the interactions *in vivo*, such as molecular crowding and the presence of nucleic acids, these experiments clearly indicate an increased binding affinity in the dark state.

Crystal Structure of the ground state of BlsA.

The resulting physiological changes that are regulated by BLUF domain proteins are controlled by the action of a separate, fused, domain or a distinct binding partner. As such, photoactivation involves an intraprotein signal transduction event and, in the case of small BLUF proteins, an interprotein signal transduction event. Upon photoexcitation, the electronic changes that occur at and around the flavin in the BLUF domain must be transmitted to the variable domain (intraprotein) and then on to the output domain or binding partner (interprotein). In order to identify features of BlsA that dictate binding interactions and as a basis for study of intra-and inter-protein signaling mechanisms, we solved the X-ray crystal structure of this protein. We purified the hexahistidine-tagged variant of BlsA and purified this protein to homogeneity. While it has been reported that BlsA may be present as both a monomer and multimer in solution [18], our gel filtration results were consistent with a monomer as the sole observed species (Figure 4A). There was one molecule of BlsA per asymmetric unit and the protein appeared to be monomeric. This was supported by analysis by the PDBePISA server [37], which did not predict any interactions that would result in stable quaternary structures. The data collection and refinement statistics are provided in Table 1. Note that electron density was not observed for the C-terminal 5 amino acids and, as such, these were not built into the model.

Author Manuscript Author Manuscript Author Manuscript Author Manuscript

Consistent with other BLUF domain proteins, BlsA has a 5-stranded β-sheet sandwiched between two pairs of helices (Figure 5A). The flavin chromophore is bound between the highly conserved N-terminal pair of helices while the C-terminal pair of helices make up the presumed protein binding domain. As observed in other BLUF domains, the conserved Y7, Q51, and M94 residues coordinate the isoalloxazine moiety of the flavin (Figure 5B). Note that, based on the absorption spectra of BlsA in solution (Figure 4B) the flavin chromophore is intact and shows the complete photocycle. However, we did not observe the electron density in the model for the AMP moiety, likely because it was freely moving in the crystals, and, as such, modeled the chromophore as FMN (Figure 5B). The orientation of the Y7 and Q51 sidechains of BlsA show similar hydrogen bonding interactions to those observed in *O. acuminata* photoactivated adenylate cyclase (OaPAC) BLUF domain [10], with Y7 making a key hydrogen bonding interaction with Q51 (Figure 5B). A superposition of BlsA with the *Synechocystis sp*. BLUF PixD (2HFN; RMSD=1.18 Å), and the BLUF domain of OaPAC (4YUS; RMSD=1.29 Å) show a high degree of structural conservation in the N-terminal BLUF domain (Figure S7A). As expected, the C-terminal region of these proteins is highly variable, presumably to accommodate distinct output domains or binding partners. Not surprisingly, considering the high degree of sequence conservation around for the flavin binding site, the residues that coordinate the chromophore are also structurally conserved (Figure S7B). The orientations of the Tyr and Gln residues, in particular, are consistent with the proposed photoactivation mechanism [10, 20, 38, 39].

Crystal structure of photo-activated state of BlsA.

Because of the nature of the flavin chromophore, BLUF-domain proteins exhibit a characteristic red-shift upon photoactivation [22, 39]. Our recombinant hexahistidine-tagged BlsA and TRX-BlsA, as expressed, exhibit an identical 12 nm red shift from 460 to 472 nm region when photoactivated with blue light (Figure 4A and Figure S6). The protein returns to the ground state with a half-life of approximately 8 minutes (Figure S8). This is consistent with previous studies of the BlsA photocycle and other BLUF domain proteins [6, 19, 20, 39], suggesting that the protein we expressed is fully active and capable of undergoing the complete photocycle. Prior spectroscopic studies have yielded great insight into the structural dynamics of BlsA immediately upon photoactivation, particularly in the region around the chromophore [20, 22, 24]. Very little, however, is yet known about large-scale protein structural changes that result from the photoexcitation event, or how these changes impact interactions with the output partner(s). To determine what structural changes of the protein result from photoexcitation we illuminated BlsA protein crystals with blue light for 30 seconds immediately prior to flash freezing these crystals in liquid nitrogen, and solved the X-ray crystal structure. Note that, other than the illumination with blue light, these crystals were grown, harvested, cryoprotected and frozen in exactly the same manner as the crystals used for the ground state structure. To ensure that the photocycle was not disrupted by crystallization, we collected the absorption spectra of BlsA protein crystals in the dark and after illumination with blue light (Figure 4B). As expected, we observe a similar red shift *in crystallo* as observed in solution.

The crystals of BlsA, after photoactivation, also diffracted well (refined to 1.76 Å) but indexed in a different space group ($P2_1$, with two molecules in the asymmetric unit) than

Author Manuscript Author Manuscript Author Manuscript Author Manuscript

that of the ground state (*C*2, one molecule in the asymmetric unit). Note that, to confirm that the change in space group was indeed attributable to light-induced changes, several crystals were harvested, from different crystallization trials, and flash frozen in the dark or after exposure to blue light. All data sets collected without photoactivation indexed in the *C*2 spacegroup, while all those exposed to light indexed in the $P2_1$ spacegroup. A comparison of the ground state to the photoactivated state shows structures reveal several significant differences. Superposition of the two structures (RMSD 0.24 Å) reveals that, while there is little variation in the BLUF domain, the two helices that make up the variable domain undergo a substantial conformational change (Figure 6A). Most of the sidechains on these helices translate between 1 and 4 Å from dark to light and some move as much as 6 Å. In addition, 11 residues of the C-terminus become unstructured and are not visible in the electron density for the photoactivated sample (Figure 6A). This may be due to a subtle translation of the variable domain that shifts the residues in the C-terminal loop 0.3 Å towards the variable domain. It is also important to note that both in this structure and the dark state structure of BlsA, the protein is observed as a monomer, consistent with our size exclusion choromatography results (Figure 4A).

The region of the protein around the flavin (Figure 6B) remains relatively unchanged between the two structures. However, a very subtle rotation of the flavin, with respect to the protein, is observed (Figure S9A). While this small change is not significant enough to justify definitive conclusions, this type of rotation is similar to what is seen in the *Oscillatoria acuminata* (OaPAC) BLUF domain [10]. The flavin in OaPAC rotates ~ 8° which significantly changes the hydrogen bonding network between it and the sidechains of Q48 and Y6. In BlsA, the rotation is only ~ 2°, and no hydrogen bond changes more than 0.1 Å (Figure S9B). Spectroscopic data on BlsA and OaPAC suggest that a likely photoactivation mechanism involves the potential formation of an excited biradical followed by immediate tautomerization of the Gln sidechain (Q51 in BlsA) [10, 20, 40]. This tautomerization drives a change in the hydrogen bonding network. While the differences observed between the ground and photoactivated structure are slight, the change in inter-atom distance between Q51 and Y7 in BlsA do indicate a slightly stronger bond and, as such, are consistent with the proposed tautomerization mechanism.

Proposed intra- and inter-protein signal transduction mechanisms.

In order to convert the photoexcitation event into a structural change that ultimately leads to the biological output, BLUF-domain proteins must transduce the incoming signal at the flavin to the distal variable domain of the protein. One hypothesis put forth to explain the intramolecular signal transduction mechanism involves the positional swapping of a Met (equivalent to M94 in BlsA) and a Trp (equivalent to W92 in BlsA) sidechain. While there is strong evidence that both the Trp and Met residues play important roles in the overall photo-cycle it is still unclear what their function may be. For the *Synechocystis sp.* BLUF domain protein, PixD, fluorescence, FTIR, and structural studies suggested that Trp91 and Met93 undergo significant conformational changes in response to light [16, 17, 41–43]. For the *R. sphaeroides* BLUF domain, AppA, photoexcitation is believed to cause disruption of the hydrogen bond between Q63 and W104. This results in movement of the sidechain of W104, which then switches position with the sidechain of M106 [44–47]. The

Author Manuscript Author Manuscript Author Manuscript Author Manuscript

position of the Trp residue at the end of the β5 strand suggest that it may be a gateway to drive intramolecular signal transfer. There is still some disagreement in the literature as to the position of sidechains and degree of solvent exposure throughout the photocycle, however variations attributed to differently truncated constructs likely account for some of the observations [19, 48–51].

While the flipping of the Trp and Met residues is believed to drive the initial intradomain signaling in some BLUF domain proteins, the Trp and Met residues in BlsA do not appear to undergo any kind of noticeable structural or positional change from dark to light (Figure 6B). In the case of BlsA, M94 interacts directly with the flavin while W92 is solvent exposed in both the ground state and photoactivated state (Figure 6B). In addition, the structures of BlsA do not reveal any obvious hydrogen bonding network between the flavin and the moving residues in the variable domain. Close examination of the structures, however, reveals a series of aromatic residues that appears to bridge these two regions of the protein (Figure S10). In fact, BlsA contains a disproportionately high percentage of Phe residues; greater than 7% of the total number of amino acids are Phe residues. In addition, there are three separate FF motifs that occur in the sequence of BlsA, two of which fall within the variable domain (Figure S11). These includes Phe49-Phe50, which projects on both sides of the β-sheet of the BLUF domain and makes direct interactions both with the flavin (F49, Figs. 5B and S9) and F128 on one of the moving helices of the variable domain (Figure S11). While the intraprotein signaling mechanism in BlsA still needs to be more fully characterized, our structural results suggest an alternative intraprotein signal transduction mechanism that may be in operation in BlsA. Upon photoactivation, electronic changes of the flavin and tautomerization of Q51 would lead to a slight rotation of the flavin and subtle shift of some of the coordinating residues, including F49 (0.2 Å average difference observed between sidechain atoms of light and dark state structures of BlsA). This movement would be propagated through the protein *via* a concomitant shift in F50 (0.3 Å average difference) and through a perpendicular π-stacking interaction with F128 (0.4 Å average difference) on one of the helices of the variable domain. F128 is part of another FF motif in BlsA (with F127), and these two residues interact with another FF pair on the other moving helix of the variable domain (F106 and F107). In the BlsA structures, the final displacement of the F106 and F107 sidechains from the light to dark structures are 1.5 Å and 1.9 Å, respectively. There are certainly additional interactions that contribute to the conformational change observed in BlsA but, from our data, it is likely that these changes are driven predominantly by aromatic and hydrophobic residues.

The final stage of signal propagation involves the interprotein signal transduction between the BLUF domain protein and its binding partner. In BlsA, the observed conformational changes in the variable domain suggest a mechanism whereby the physicochemical properties on the surface of that region of the protein dictate the interaction with the binding partner. In order to test this hypothesis, we conducted a protein-protein docking experiment using the ZDOCK server [52]. We used the dark state structure of BlsA and the dimeric form of the *V. cholera* Fur protein (2W57; 58% sequence identity to *A. baumannii* Fur) as starting models. While nearly all of the docking results placed the variable domain of BlsA near to, or directly interacting with, the highly basic DNA binding region of Fur, the lowest energy state had one of the variable domain helices located directly in the DNA

Author Manuscript Author Manuscript Author Manuscript Author Manuscript

binding pocket of Fur (Figure 7A). An examination of the surface charge of BlsA and Fur (Figure 7B) shows clear electronegative character on the surface of the BlsA. Similarly, the DNA-binding 'lobes' of Fur are highly electropositive in nature. Thus, the electronegative variable domain of BlsA can putatively interact with the electropositive DNA binding domain of Fur. Superposition of the photoactivated state of BlsA onto the dark state in the BlsA-Fur complex (Figure 7C) reveals that the conformational change that occurs in the variable domain would create numerous clashes between BlsA and Fur (Figure 7D). While the C-terminus of BlsA was unresolved in our photoactivated structure, it was recently suggested that this region of the protein may also play a role in interacting, particularly through electrostatic interactions, with the binding partner [53]. Overall, our structural and docking results suggest a putative mechanism whereby BlsA interacts with its transcription factor binding partner, in its ground state, through an electrostatic interaction in the DNA binding pocket and that, upon photoactivation, the conformational change in the variable domain causes the dissociation of BlsA. This is consistent with previous studies of the regulation of Fur by BlsA, which suggest that Fur transcription is inhibited in the dark and enhanced by photoactivated BlsA [7, 18, 19]. We cannot rule out, however, the possibility that BlsA and Fur make a more stable complex *in vivo* and that subtle conformational changes in BlsA alter the affinity of this complex for DNA without BlsA fully dissociating.

As a means to test this mechanism, we generated a truncated form of BlsA, lacking a helix (residues 101–110) in the variable domain. We then repeated MST experiments to compare the binding of this truncated BlsA ($BlsA_{del101–110}$) to Fur. The MST data shows no apparent affinity between Fur and $BlsA_{del101–110}$ (Figure 8). This suggests that this helix plays some role in the interaction between BlsA and it's binding partner Fur. This proposed mechanism, whereby BlsA blocks transcription through an electrostatic interaction with the DNA binding pocket may also explain how BlsA appears to control a number of different processes in *A. baumanii* [3, 6]. The expression and activity of BlsA have also been observed to be sensitive to temperature changes [6, 18]. These observations may be simply a result of temperature effects on binding affinity, or may suggest the presence of other regulatory factors. Further studies will be needed to address these nuances of the photoregulation mediated by BlsA.

The opportunistic pathogen, *A. baumannii*, is responsible for a wide variety of infections that can be very difficult to treat, in part due to the emergence of drug-resistant strains. The photoreceptor, BlsA, modulates a variety of *A. baumannii* physiological functions, and has been implicated in biofilm formation and overall virulence. In this work, we have identified a new binding partner of this protein, BfmR, that provides a direct link between photoreception and biofilm formation. In addition, our structural studies provide critical insights into how the light-induced conformational changes that occur in BlsA drive both intra- and interprotein signal transduction. Considering the importance of light to *A. baumannii* viability and virulence, these data may provide a framework for the development of novel therapeutics that disrupt photoregulation in this organism.

Author Manuscript Author Manuscript Author Manuscript Author Manuscript

METHODS

Protein Expression and Purification.

BlsA from *Acinetobacter baumannii* was expressed with an N-terminal histidine tag as either a pET15 (Novagen) construct (p15_BlsA) or a pDB.His.TRX (DNASU) construct with a recombinant thioredoxin fusion (Trx_BlsA). BfmR and Fur from *Acinetobacter baumannii* were expressed with an N-terminal histidine tag from a modified pET-28 vector, pTHT, that has a tobacco etch virus protease recognition site in place of the thrombin site. To express BlsA, BfmR or Fur protein, *E. coli* Bl21 (DE3) were transformed with p15_BlsA, pDB.His.TRX_BlsA, pTHT_BfmR, or pTHT_Fur and plated on LB-agar containing 50 μg/mL ampicillin, or on LB-agar containing 50 μg/mL kanamycin, as appropriate. Overnight cultures were prepared by inoculating LB Miller broth, containing 50 μg/mL ampicillin or kanamycin, with single colony and incubating at 37 °C with vigorous shaking. Large scale cultures were prepared by inoculating 1 L of LB broth (BfMR, Fur) or 2XYT media broth (BlsA) with 50 μg/mL ampicillin or kanamycin with 10 mL of the overnight culture. The cultures were incubated at 37 °C with shaking at 250 rpm until an O.D of ~0.4 was obtained, then the temperature was lowered to 18°C. Once the O.D. was between 0.6–0.7, 100 μM isopropyl β-D-1-thiogalactopyranoside (IPTG) was added to induce protein expression and the culture was further incubated with shaking for an additional 14 hours. Cells were harvested by centrifugation at 4°C for 20 minutes at 6000*g* and the cell pellet was stored at −20°C.

Pellets were resuspended in lysis buffer (50 mM Tris base, pH 7.5, 500 mM sodium chloride, 10 mM imidazole, 10 % glycerol) and lysed by sonication. The lysate was cleared by centrifugation at 25 000*g* for 60 minutes at 4°C. All proteins were purified using immobilized metal affinity chromatography (IMAC) followed by anion exchange. Briefly, the clear lysate was run through a Ni-NTA column (Qiagen) equilibrated with lysis buffer followed by a wash with lysis buffer containing 10 mM imidazole. The protein was then eluted with lysis buffer containing 350 mM imidazole. The eluted proteins were buffer exchanged into 50 mM Tris base, pH 9, for anion exchange. Anion exchange was performed by using a HiTrap Q HP column (GE). The proteins were loaded and then washed with 50 mM Tris base, pH 9, and 20–150 mM NaCl (20 mL of 20 mM NaCl for p15_BlsA, 50 mL of 150 mM NaCl for pDB.His.TRX_BlsA, pTHT_BfmR and pTHT_Fur). BlsA (p15_BlsA) was eluted with 150 mM NaCl, Trx-BlsA (pDB.His.TRX_BlsA) was eluted with 200 mM NaCl, and BfMR or Fur were eluted with 250 mM NaCl. To further purify BlsA (p15_BlsA) an additional size exclusion step (superdex 200 10/300 GL, GE), using 20 mM Tris base, pH 7.5, and 150 NaCl, was performed. Protein concentrations were determined using the Bradford assay and protein purity was estimated by SDS_PAGE analysis. For storage, BlsA (p15_BlsA) was buffer-exchanged into 20 mM Tris base, pH 7.5, 30 mM NaCl, then flash frozen with liquid nitrogen and stored at −80°C. TRX-BlsA (pDB.His.TRX_BlsA), BfmR (pTHT_BfmR) and Fur (pTHT_Fur) were buffer exchanged into 20 mM HEPES, pH 8, 150 mM NaCl, then flash frozen with liquid nitrogen and stored at −80°C.

Author Manuscript Author Manuscript Author Manuscript Author Manuscript

Immunoprecipitation of BlsA-binding proteins.

BlsA was buffer exchanged into PBS (100 mM sodium phosphate, 150 mM sodium chloride, pH 7.4) and the protein was aliquoted into four 1 mg/mL fractions (5 μM). Several heterobifunctional cross-linking reagents (sulfo-SDA, or sulfo-LC- SDA, or sulfo-SDAD, Pierce/Thermo-Fisher), with both an amine-reactive and a photoactive end, were used in the experiment. To attach the cross-linkers to BlsA, three of the four aliquots were treated with 100 μM of amine-reactive/photoactivatable cross linkers and the fourth aliquot (control) was treated with 10 μL of 100% DMSO. All four samples were incubated in the dark on ice for 2 hours, followed by a 10 min 25°C incubation, and were then quenched with 10 μL of 1M Tris HCl, pH 8.0. Excess cross-linker were removed from the reactions by washing with 0.5 mL PBS 30 times, using a 10 kDa cutoff centrifugal filtration device (Millipore).

To make the lysate, 100 mL of *Acinetobacter baumannii* ATCC 19606 was cultured in LB media for 6 hours at 37 °C to a final OD of approximately 2. The cells were harvested by centrifugation at 4°C for 15 minutes at 6000*g* and then resuspended in 30 mL of PBS. The cells were incubated with 30 μL of 30 mg/mL lysozyme for 75 minutes, and then lysed by sonication. The lysate was cleared by centrifugation for 45 minutes at 26 000*g* at 4°C. The clear lysate was aliquoted, in 1 mL fractions, into 20 glass tubes and then exposed to LED blue light (455 nm) for 1 minute.

For each of the 3 sets of cross-linker treated BlsA, 200 μL of BlsA were added to 1mL of *A.baumannii* lysate for a total of 4 tubes per one cross linker. Two sets of four tubes with *A. baumannii* lysate per set of negative controls were prepared. One set contained *A. baumannii* lysate, cross linker and no BlsA, while the other set was composed of *A. baumannii* lysate and DMSO treated BlsA. To bring the final volume to 1.5 mL, 300 μL of PBS was added to all the tubes. All of the samples were then exposed to blue light for 1 minute. The samples were split in half such that 2 of every cross-linker containing sample, and 2 of each negative control set were designated to either light or dark condition. Designated dark condition samples were kept in a sealed container to prevent exposure to light, and the light condition samples were exposed to blue light (455nm) throughout the process. All samples were then irradiated with a UV lamp (365 nm) for 15 min, to activate the cross-linking chemistry, during which time the samples were subjected to gentle shaking.

To identify BlsA binding partners, the 6-His-tagged BlsA was isolated *via* batch purification with the anti-his affinity resin (GenScript). All 20 samples were incubated with 70 μL of PBS equilibrated anti-his affinity resin at 25°C for 90 minutes. The resin was washed using a centrifugal filter, 3 times, with 1 mL of PBS. The resin was then incubated in PBS for 30 min for the first wash and 10 min for subsequent washes. This was followed by 3 further washes with 1 mL of 750 mM NaCl. BlsA protein complex was eluted from the beads with 400 μL of 100 mM Tris, 500 mM NaCl, pH 12.0, and then neutralized with 2.5 μL of 1 M HCl. This was followed by a second elution round of 250 μL pH 12 buffer, which was neutralized with 1.20 μL of 1M HCl. The samples were flash frozen and stored at −20°C. The frozen samples were sent out for trypsin digest and standard protein identification by mass spectrometry (Stony Brook Proteomics Facility). Briefly, thawed samples were incubated with 0.1% TFA, 5% methanol to release bound proteins and dried by centrifugal lyophilization. Proteins were reduced, alkylated, and digested with trypsin. The resulting

Author Manuscript Author Manuscript Author Manuscript Author Manuscript

peptide extract was dried and dissolved in 0.1% formic Acid (FA) (buffer A) for analysis by LC-MS/MS using 5u ProntoSil 120–5-C18H column (0.1 × 10cm) running at 300 nL min^{-1}. The peptides were eluted from the column by applying a 115 min gradient from 2% buffer B (98% ACN, 0.1% FA) to 40% buffer B. The gradient was switched from 40% to 80% buffer B over 3 min and held constant for 3 min. Finally, the gradient was changed from 80% buffer B to 2% buffer B over 0.1 min, and then held constant at 2% buffer B for 29 more minutes. The application of a 2.2 kV distal voltage electrosprayed the eluting peptides directly into an LTQ Orbitrap XL ion trap mass spectrometer (Thermo). Full mass spectra (MS) were recorded on the peptides over a 400 to 2000 m/z range at 60,000 resolution, followed by top-five MS/MS scans in the ion-trap. Charge state dependent screening was turned on, and peptides with a charge state of +2 or higher were analyzed. MS/MS spectra were extracted from the RAW file with ReAdW.exe (http://sourceforge.net/projects/sashimi). The resulting mzXML data files were searched with the GPM X!Tandem and MaXQuant Andromeda search engines.

Microscale Thermophoresis Analysis.

BlsA and TRX-BlsA were fluorescently labeled using the Monolith Protein Labeling Kit RED NHS (Nanotemper) according to manufacturer's instructions. Labeled protein was diluted to a range of 20 nM - 50 nM in MST buffer (20 mM HEPES pH 8, 150 mM NaCl, 0.01% Tween-20) and centrifuged for 5 min at 14,500*g* at 4 °C. BfmR or Fur were added to a PCR tube and then serially diluted (2-fold) with MST buffer for 15 tubes. Labeled BlsA, TRX-BlsA or control (10 μL) was mixed with the diluted unlabeled proteins. The samples were incubated for 4 minutes in the dark, centrifuged for 1 minute, then loaded into MST NT.115 standard glass capillaries (Nanotemper). Binding experiments were carried out on the Monolith NT.115 red channel with 20–40% MST power and 10–20% LED power depending on the fluorescence signal of the labeled protein. The dissociation constant (K_D) was calculated by fitting the data using the one site, nonspecific total fit in Prism (GraphPad). For each experiment, the curves were fit to data that were the average of three replicates. For the MST controls, the same protocol was used and binding experiments were conducted with labeled control proteins bovine serum albumin (BSA) or thioredoxin (TRX) with unlabeled BlsA, TRX-BlsA, BfmR or Fur, and using labeled TRX-BlsA with unlabeled control proteins.

Crystallization and Data Collection.

For crystal trials, hexahistidine-tagged BlsA was used, without removal of the tag, at 8 – 15 mg/mL. Sparse matrix screening (Peg/Ion and Crystal Screen, Hampton) using the hanging drop vapor diffusion method was employed to identify the initial crystallization conditions for BlsA. The hanging drop consisted of 1.25 μL of well reservoir and 1.25 μL of BlsA (p15_BlsA; 330 uM). The trays were incubated at 20°C for a month before clusters of needle-shaped crystals of BlsA appeared in a condition containing 0.2 M sodium chloride and 20% w/v Polyethylene glycol 3,350. With microseeding, crystal growth was accelerated to one week in the same condition. Crystals were harvested in ambient light and serially introduced into cryoprotectant composed of well reservoir and NaCl. The initial NaCl concentration was 0.1 M and was serially increased to 2 M NaCl. After equilibration in well solution with 2M NaCl, crystals were flash frozen in liquid nitrogen. To obtain the

Author Manuscript Author Manuscript Author Manuscript Author Manuscript

activated state, a subset of crystals was exposed to blue light (455 nm) for 30 seconds just prior to flash freezing. Data was collected at 100 K at North Eastern Collaborative Access Team (NE-CAT) beamline 24-ID-C (ground state) on a Dectris Pilatus 6MF detector and at 17-ID-1 (AMX) at National Synchrotron Light Source II (NSLSII) on an Eiger 9M detector for the photoactivated state protein. The data collection statistics are provided in Table 1.

Structure Determination and Refinement.

The data were indexed, integrated and scaled using XDS [54], and Aimless [55]. The BlsA structure was initially determined by molecular replacement using phenix.phaser-MR [56] with the *Synechocystis sp.* protein structure (PDB entry 3MZI, 35% sequence identity) as a search model. The model was initially refined without the ligand using iterative rounds of manual model building with Coot [57] and restrained refinement with phenix.refine or REFMAC5 [58]. After the refinement converged, the Flavin component of the FAD co-factor was fit in the ordered electron density and water molecules were added using Coot. After an additional round of refinement, the remainder of the FMN and several additional water molecules were added. The data refinement statistics are provided in Table 1.

On-column protein interaction experiments.

To determine if the interaction of BlsA with Fur or BfmR was light dependent, we conducted on an-column interaction experiment. Three sets of samples were generated containing hexahistidine-tagged BlsA (100 μL of 0.6 mg/mL) and either 100 μL of buffer (50 mM sodium phosphate, 150 mM sodium chloride, and 15 mM imidazole, pH 7.6), 100 μL of untagged BfmR (0.3 mg/mL) or μL of untagged Fur (0.3 mg/mL). One set of these 3 samples was incubated for 30 minutes in the dark, while the other set was incubated for 30 minutes while being exposed to blue light (455 nm). After the incubation, 50 uL of Ni-NTA slurry (Qiagen) was added to each sample and incubated for an additional 10 minutes in dark or light. The samples were centrifuged at 2,000 g for 2 minutes to pellet the resin. The supernatant, representing the unbound proteins (flowthrough), was removed and saved for analysis. To wash the resin, 100 μL of buffer was added, the resin was rocked for 5 minutes and then centrifuged, as above, to pellet the resin. This wash supernatant was added to the flowthrough fraction. To elute the bound proteins, 200 μL of elution buffer with 300 mM imidazole was added and the sample was rocked for 5 minutes before centrifugation at 2,000 g for 2 minutes to pellet the resin. This supernatant, representing the bound proteins (elution fraction) was saved for analysis. To analyze which proteins bound, the flowthrough and elution samples for both the dark and light experiments for the BlsA:buffer, BlsA:Fur, and BlsA:BfmR were run on an SDS-PAGE gel. Quantification of gel band intensity was carried out using the ImageLab software (Qiagen) to estimate the ratio of dark:light binding affinity (Fig. S5).

Protein-protein Docking.

For initial docking experiments we used the ground state structure of BlsA and the *V. cholera* Fur protein (2W57; 58% sequence identity over 92% of the sequence to the *A. baumannii* Fur protein) without further modification. A single monomer was used for BlsA while the Fur structure was used in the dimeric form. Docking was performed by Fast Fourier Transform-based protein docking using the ZDOCK server running ZDOCK version

Author Manuscript Author Manuscript Author Manuscript Author Manuscript

3.0.2 [52]. The server output the top 10 predictions, based on a scoring function that includes shape complementarity, electrostatics, and a pairwise statistical potential [59, 60]. To compare the fit of the photo-activated BlsA structure to the Fur protein, we superimposed the photo-activated BlsA structure onto the docked ground state BlsA structure using an all-atom alignment in PyMol.

Supplementary Material

Refer to Web version on PubMed Central for supplementary material.

ACKNOWLEDGEMENTS AND FUNDING

JI and JTC would like to acknowledge the Stony Brook Chemical Biology Training Program (T32GM092714), and the Stony Brook IMSD-MERGE Program (R25GM103962), respectively, for training support. This work was supported by the National Science Foundation through award numbers MCB-1750637 (JBF) and MCB-1817837 (PJT), and by the Research Corporation for Science Advancement through a Cottrell Scholar award to J. French. The content is solely the responsibility of the authors and does not necessarily represent the official views of any of the funding agencies.

Note that the structures reported herein have been deposited to the protein data bank with PDB codes 6W6Z (ground state) and 6W72 (photoactivated state).

ABBREVIATIONS

BLUF	blue light using Flavin
BlsA	blue light sensing A
BfmR	biofilm master regulator
CoIP	co-Immunoprecipitation
FAD	flavin adenine dinucleotide
FMN	flavin mononucleotide
FTIR	Fourier-transform infrared spectroscopy
Fur	ferric uptake regulator
IMAC	Immobilized metal affinity chromatography
MST	microscale thermophoresis
OaPAC	*Oscillatoria acuminate* photoactivated adenylate cyclase
TRX	thioredoxin

REFERENCES

1. Longo F, Vuotto C, and Donelli G, Biofilm formation in Acinetobacter baumannii. New Microbiol, 2014. 37(2): p. 119–27. [PubMed: 24858639]
2. McConnell MJ, Actis L, and Pachon J, Acinetobacter baumannii: human infections, factors contributing to pathogenesis and animal models. FEMS Microbiol Rev, 2013. 37(2): p. 130–55. [PubMed: 22568581]

Author Manuscript Author Manuscript Author Manuscript Author Manuscript

3. Muller GL, et al. , Light Modulates Metabolic Pathways and Other Novel Physiological Traits in the Human Pathogen Acinetobacter baumannii. J Bacteriol, 2017. 199(10): p. e00011–17. [PubMed: 28289081]
4. Pezza A, et al. , Through the eyes of a pathogen: light perception and signal transduction in Acinetobacter baumannii. Photochem Photobiol Sci, 2019. 18(10): p. 2363–2373. [PubMed: 31290528]
5. Wood CR, et al. , A Light-Regulated Type I Pilus Contributes to Acinetobacter baumannii Biofilm, Motility, and Virulence Functions. Infect Immun, 2018. 86(9): p. e00442–18. [PubMed: 29891547]
6. Mussi MA, et al. , The opportunistic human pathogen Acinetobacter baumannii senses and responds to light. J Bacteriol, 2010. 192(24): p. 6336–45. [PubMed: 20889755]
7. Golic AE, et al. , BlsA Is a Low to Moderate Temperature Blue Light Photoreceptor in the Human Pathogen Acinetobacter baumannii. Front Microbiol, 2019. 10: p. 1925. [PubMed: 31497002]
8. Lindner R, et al. , Photoactivation Mechanism of a Bacterial Light-Regulated Adenylyl Cyclase. J Mol Biol, 2017. 429(9): p. 1336–1351. [PubMed: 28336405]
9. Masuda S and Bauer CE, AppA is a blue light photoreceptor that antirepresses photosynthesis gene expression in Rhodobacter sphaeroides. Cell, 2002. 110(5): p. 613–23. [PubMed: 12230978]
10. Ohki M, et al. , Molecular mechanism of photoactivation of a light-regulated adenylate cyclase. Proc Natl Acad Sci U S A, 2017. 114(32): p. 8562–8567. [PubMed: 28739908]
11. Winkler A, et al. , A ternary AppA-PpsR-DNA complex mediates light regulation of photosynthesis-related gene expression. Nat Struct Mol Biol, 2013. 20(7): p. 859–67. [PubMed: 23728293]
12. Kanazawa T, et al. , Biochemical and physiological characterization of a BLUF protein-EAL protein complex involved in blue light-dependent degradation of cyclic diguanylate in the purple bacterium Rhodopseudomonas palustris. Biochemistry, 2010. 49(50): p. 10647–55. [PubMed: 21082778]
13. Masuda S, Light detection and signal transduction in the BLUF photoreceptors. Plant Cell Physiol, 2013. 54(2): p. 171–9. [PubMed: 23243105]
14. Okajima K, et al. , Biochemical and functional characterization of BLUF-type flavin-binding proteins of two species of cyanobacteria. J Biochem, 2005. 137(6): p. 741–50. [PubMed: 16002996]
15. Stierl M, et al. , Light modulation of cellular cAMP by a small bacterial photoactivated adenylyl cyclase, bPAC, of the soil bacterium Beggiatoa. J Biol Chem, 2011. 286(2): p. 1181–8. [PubMed: 21030594]
16. Masuda S, et al. , Crucial role in light signal transduction for the conserved Met93 of the BLUF protein PixD/Slr1694. Plant Cell Physiol, 2008. 49(10): p. 1600–6. [PubMed: 18772185]
17. Yuan H and Bauer CE, PixE promotes dark oligomerization of the BLUF photoreceptor PixD. Proc Natl Acad Sci U S A, 2008. 105(33): p. 11715–9. [PubMed: 18695243]
18. Tuttobene MR, Cribb P, and Mussi MA, BlsA integrates light and temperature signals into iron metabolism through Fur in the human pathogen Acinetobacter baumannii. Sci Rep, 2018. 8(1): p. 7728. [PubMed: 29769610]
19. Abatedaga I, et al. , Integration of Temperature and Blue-Light Sensing in Acinetobacter baumannii Through the BlsA Sensor. Photochem Photobiol, 2017. 93(3): p. 805–814. [PubMed: 28500705]
20. Brust R, et al. , Ultrafast Structural Dynamics of BlsA, a Photoreceptor from the Pathogenic Bacterium Acinetobacter baumannii. J Phys Chem Lett, 2014. 5(1): p. 220–224. [PubMed: 24723998]
21. Brust R, et al. , Proteins in action: femtosecond to millisecond structural dynamics of a photoactive flavoprotein. J Am Chem Soc, 2013. 135(43): p. 16168–74. [PubMed: 24083781]
22. Fujisawa T and Masuda S, Light-induced chromophore and protein responses and mechanical signal transduction of BLUF proteins. Biophys Rev, 2018. 10(2): p. 327–337. [PubMed: 29235080]
23. Lukacs A, et al. , Photoexcitation of the blue light using FAD photoreceptor AppA results in ultrafast changes to the protein matrix. J Am Chem Soc, 2011. 133(42): p. 16893–900. [PubMed: 21899315]

Author Manuscript Author Manuscript Author Manuscript Author Manuscript

24. Lukacs A, et al. , BLUF domain function does not require a metastable radical intermediate state. J Am Chem Soc, 2014. 136(12): p. 4605–15. [PubMed: 24579721]
25. Lukacs A, et al. , Excited state structure and dynamics of the neutral and anionic flavin radical revealed by ultrafast transient mid-IR to visible spectroscopy. J Phys Chem B, 2012. 116(20): p. 5810–8. [PubMed: 22515837]
26. Mathes T and Gotze JP, A proposal for a dipole-generated BLUF domain mechanism. Front Mol Biosci, 2015. 2: p. 62. [PubMed: 26579529]
27. Gallegos MT, et al. , Arac/XylS family of transcriptional regulators. Microbiol Mol Biol Rev, 1997. 61(4): p. 393–410. [PubMed: 9409145]
28. Nara F, et al. , Molecular analysis of mutant ompR genes exhibiting different phenotypes as to osmoregulation of the ompF and ompC genes of Escherichia coli. Mol Gen Genet, 1986. 202(2): p. 194–9. [PubMed: 3010044]
29. Seo SW, et al. , Revealing genome-scale transcriptional regulatory landscape of OmpR highlights its expanded regulatory roles under osmotic stress in Escherichia coli K-12 MG1655. Sci Rep, 2017. 7(1): p. 2181. [PubMed: 28526842]
30. Yang J, Tauschek M, and Robins-Browne RM, Control of bacterial virulence by AraC-like regulators that respond to chemical signals. Trends Microbiol, 2011. 19(3): p. 128–35. [PubMed: 21215638]
31. Laub MT and Goulian M, Specificity in two-component signal transduction pathways. Annu Rev Genet, 2007. 41: p. 121–45. [PubMed: 18076326]
32. Tomaras AP, et al. , Characterization of a two-component regulatory system from Acinetobacter baumannii that controls biofilm formation and cellular morphology. Microbiology, 2008. 154(Pt 11): p. 3398–3409. [PubMed: 18957593]
33. Geisinger E, et al. , A global regulatory system links virulence and antibiotic resistance to envelope homeostasis in Acinetobacter baumannii. PLoS Pathog, 2018. 14(5): p. e1007030. [PubMed: 29795704]
34. Russo TA, et al. , The Response Regulator BfmR Is a Potential Drug Target for Acinetobacter baumannii. mSphere, 2016. 1(3): p. e00082–16. [PubMed: 27303741]
35. Umland TC, et al. , In vivo-validated essential genes identified in Acinetobacter baumannii by using human ascites overlap poorly with essential genes detected on laboratory media. mBio, 2012. 3(4): p. e000113–12.
36. Tanaka K, et al. , Light-induced conformational change and transient dissociation reaction of the BLUF photoreceptor Synechocystis PixD (Slr1694). J Mol Biol, 2011. 409(5): p. 773–85. [PubMed: 21530536]
37. Krissinel E and Henrick K, Inference of macromolecular assemblies from crystalline state. J Mol Biol, 2007. 372(3): p. 774–97. [PubMed: 17681537]
38. Gil AA, et al. , Photoactivation of the BLUF Protein PixD Probed by the Site-Specific Incorporation of Fluorotyrosine Residues. J Am Chem Soc, 2017. 139(41): p. 14638–14648. [PubMed: 28876066]
39. Park SY and Tame JRH, Seeing the light with BLUF proteins. Biophys Rev, 2017. 9(2): p. 169–176. [PubMed: 28510088]
40. Domratcheva T, et al. , Evidence for Tautomerisation of Glutamine in BLUF Blue Light Receptors by Vibrational Spectroscopy and Computational Chemistry. Sci Rep, 2016. 6: p. 22669. [PubMed: 26947391]
41. Kraft BJ, et al. , Spectroscopic and mutational analysis of the blue-light photoreceptor AppA: a novel photocycle involving flavin stacking with an aromatic amino acid. Biochemistry, 2003. 42(22): p. 6726–34. [PubMed: 12779327]
42. Masuda S, et al. , The critical role of a hydrogen bond between Gln63 and Trp104 in the blue-light sensing BLUF domain that controls AppA activity. J Mol Biol, 2007. 368(5): p. 1223–30. [PubMed: 17399741]
43. Yuan H, et al. , Crystal structures of the Synechocystis photoreceptor Slr1694 reveal distinct structural states related to signaling. Biochemistry, 2006. 45(42): p. 12687–94. [PubMed: 17042486]

Author Manuscript Author Manuscript Author Manuscript Author Manuscript

44. Anderson S, et al. , Structure of a novel photoreceptor, the BLUF domain of AppA from Rhodobacter sphaeroides. Biochemistry, 2005. 44(22): p. 7998–8005. [PubMed: 15924418]
45. Grinstead JS, et al. , Light-induced flipping of a conserved glutamine sidechain and its orientation in the AppA BLUF domain. J Am Chem Soc, 2006. 128(47): p. 15066–7. [PubMed: 17117839]
46. Jung A, et al. , Crystal structures of the AppA BLUF domain photoreceptor provide insights into blue light-mediated signal transduction. J Mol Biol, 2006. 362(4): p. 717–32. [PubMed: 16949615]
47. Masuda S, Hasegawa K, and Ono TA, Tryptophan at position 104 is involved in transforming light signal into changes of beta-sheet structure for the signaling state in the BLUF domain of AppA. Plant Cell Physiol, 2005. 46(12): p. 1894–901. [PubMed: 16204305]
48. Dragnea V, et al. , Spectroscopic studies of the AppA BLUF domain from Rhodobacter sphaeroides: addressing movement of tryptophan 104 in the signaling state. Biochemistry, 2009. 48(42): p. 9969–79. [PubMed: 19746968]
49. Gil AA, et al. , Mechanism of the AppABLUF Photocycle Probed by Site-Specific Incorporation of Fluorotyrosine Residues: Effect of the Y21 pKa on the Forward and Reverse Ground-State Reactions. J Am Chem Soc, 2016. 138(3): p. 926–35. [PubMed: 26708408]
50. Karadi K, et al. , Functional dynamics of a single tryptophan residue in a BLUF protein revealed by fluorescence spectroscopy. Sci Rep, 2020. 10(1): p. 2061. [PubMed: 32029866]
51. Unno M, Kikuchi S, and Masuda S, Structural refinement of a key tryptophan residue in the BLUF photoreceptor AppA by ultraviolet resonance Raman spectroscopy. Biophys J, 2010. 98(9): p. 1949–56. [PubMed: 20441759]
52. Pierce BG, et al. , ZDOCK server: interactive docking prediction of protein-protein complexes and symmetric multimers. Bioinformatics, 2014. 30(12): p. 1771–3. [PubMed: 24532726]
53. Wood CR, et al. , Structural and functional analysis of the Acinetobacter baumannii BlsA photoreceptor and regulatory protein. PLoS One, 2019. 14(8): p. e0220918. [PubMed: 31415622]
54. Kabsch W, Xds. Acta Crystallogr D Biol Crystallogr, 2010. 66(Pt 2): p. 125–32. [PubMed: 20124692]
55. Evans PR and Murshudov GN, How good are my data and what is the resolution? Acta Crystallogr D Biol Crystallogr, 2013. 69(Pt 7): p. 1204–14. [PubMed: 23793146]
56. Liebschner D, et al. , Macromolecular structure determination using X-rays, neutrons and electrons: recent developments in Phenix. Acta Crystallogr D Struct Biol, 2019. 75(Pt 10): p. 861–877. [PubMed: 31588918]
57. Emsley P, et al. , Features and development of Coot. Acta Crystallogr D Biol Crystallogr, 2010. 66(Pt 4): p. 486–501. [PubMed: 20383002]
58. Murshudov GN, Vagin AA, and Dodson EJ, Refinement of macromolecular structures by the maximum-likelihood method. Acta Crystallogr D Biol Crystallogr, 1997. 53(Pt 3): p. 240–55. [PubMed: 15299926]
59. Chen R, Li L, and Weng Z, ZDOCK: an initial-stage protein-docking algorithm. Proteins, 2003. 52(1): p. 80–7. [PubMed: 12784371]
60. Mintseris J, et al. , Integrating statistical pair potentials into protein complex prediction. Proteins, 2007. 69(3): p. 511–20. [PubMed: 17623839]

Author Manuscript Author Manuscript Author Manuscript Author Manuscript

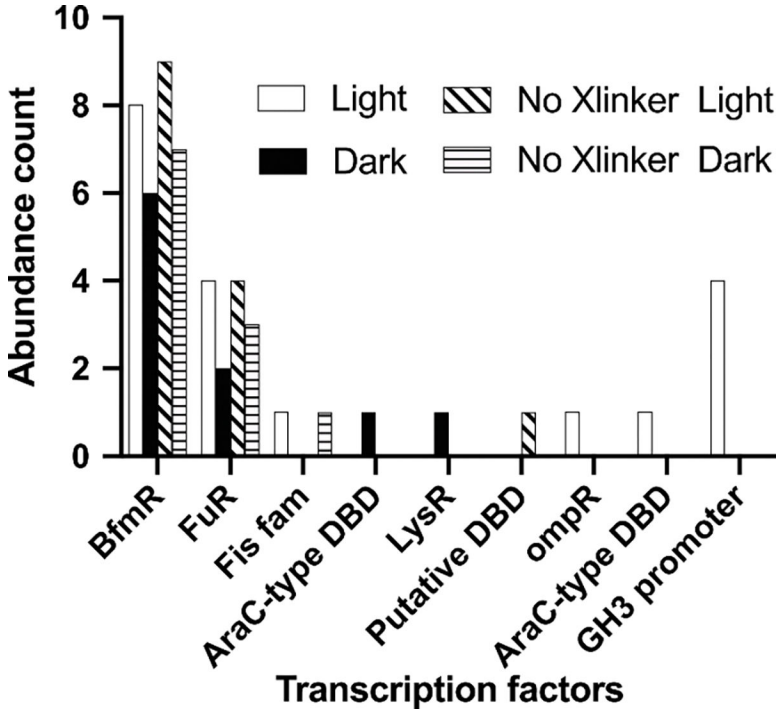

Figure 1. Co-immunoprecipitation of BlsA and its binding partners.

Immunoprecipitation of his-tagged BlsA from *A. baumannii* cell lysate revealed a number of potential binding partners. Amongst these were several transcription factors, including the biofilm regulator BfmR and the iron uptake regulator Fur. Shown are the spectral counts from the LC-MS/MS analysis of the transcription factors identified in the respective BlsA immunoprecipitation experiments. The experiments were conducted both in the presence and absence of blue light as well as with or without added chemical cross-linking reagents. The purpose of this was to broadly identify binding partners under any condition and not necessarily to distinguish light vs. dark binding partners. Both BfmR and Fur were observed under all conditions tested. All experiments were conducted in duplicate.

Author Manuscript Author Manuscript Author Manuscript Author Manuscript

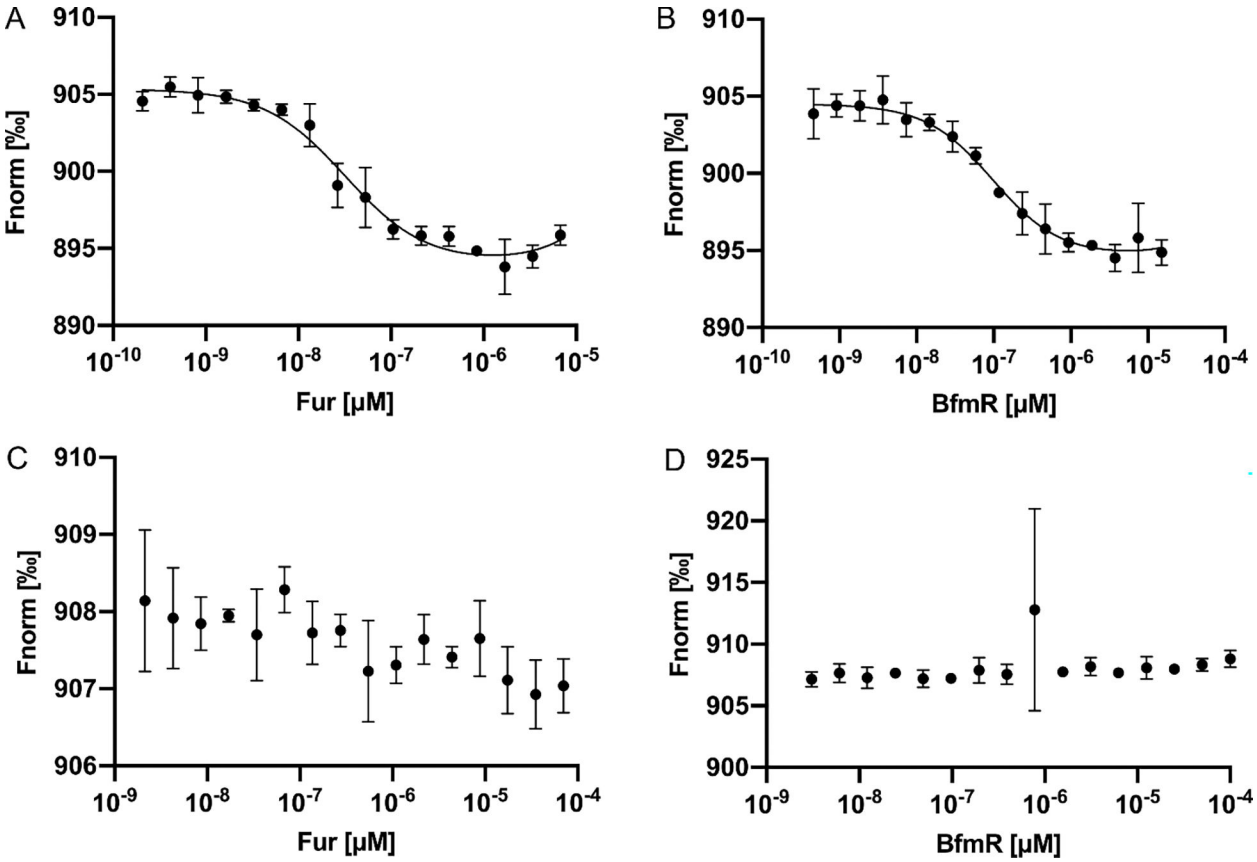

Figure 2. Quantification of interaction between BlsA and binding partners.

Microscale thermophoresis (MST) was used to quantify the binding affinity of BlsA and potential binding partners. TRX-BlsA and Fur (A) interact with a K_D of 10 nM, while TRX-BlsA and BfmR (B) have a K_D of 3 nm. No measurable interactions were observed for the control reactions, TRX with Fur (C) or TRX with BfmR (D). Additional controls are shown in Figure S3. All MST measurements were conducted in triplicate, in ambient light at 23 °C. Error bars correspond to standard deviation of the triplicate measurements.

Author Manuscript Author Manuscript Author Manuscript Author Manuscript

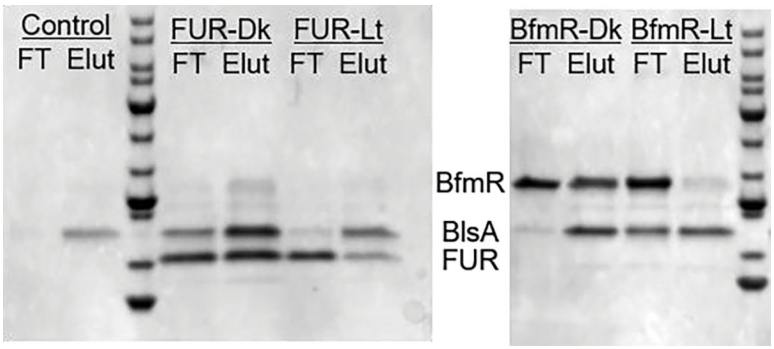

Figure 3. Light-dependent interaction between BlsA and binding partners.

To confirm that the interaction between BlsA and the binding partners BfmR and Fur was light-dependent, we used an on-column interaction assay. Samples of hexahistidine-tagged BlsA were incubated with either buffer (Control), untagged Fur, or untagged BfmR under dark (Dk) or light (Lt) conditions. After 30 minutes of incubation the solutions were run over Ni-NTA resin. The proteins that did not bind to the column were collected (FT) as was the proteins that eluted in 300 mM imidazole (Elut). Both Fur and BfmR appear to interact with BlsA in the dark (seen in the elution fraction) with a much higher affinity than when illuminated (little protein seen in the elution fractions when illuminated).

Author Manuscript Author Manuscript Author Manuscript Author Manuscript

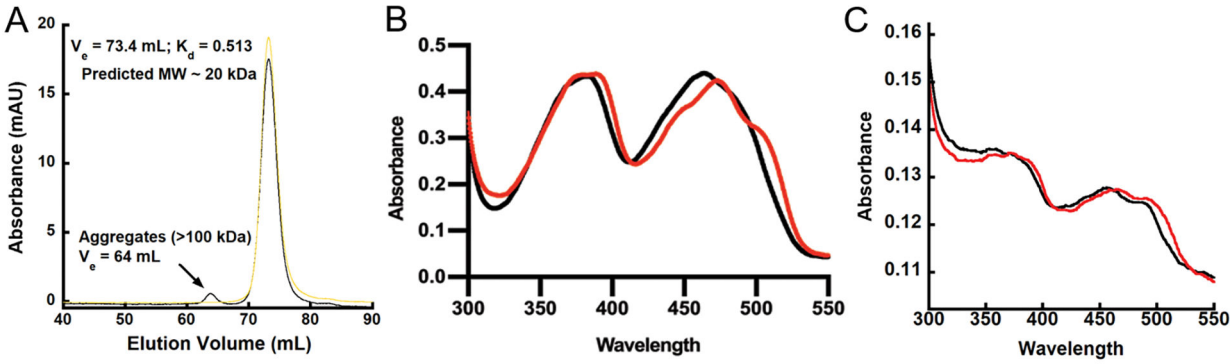

Figure 4. Absorbance spectra and size-exclusion chromatography results.

Size exclusion chromatography was carried out to characterize the oligomeric state of BlsA (A). The protein eluted as a monomer both when the SEC was carried out in the dark (grey line) or when illuminated with blue light (yellow line). The standards used and standard curve for the analysis is given in Figure S4. A comparison of the absorbance spectrum of hexahistidine-tagged BlsA in the dark state (B, black) to the spectrum collected after the protein was illuminated with blue light (B, red) shows the red shift that is characteristic of BLUF proteins. Similarly, the characteristic red shift is also seen in the absorbance spectra taken using BlsA crystals (C).

Author Manuscript Author Manuscript Author Manuscript Author Manuscript

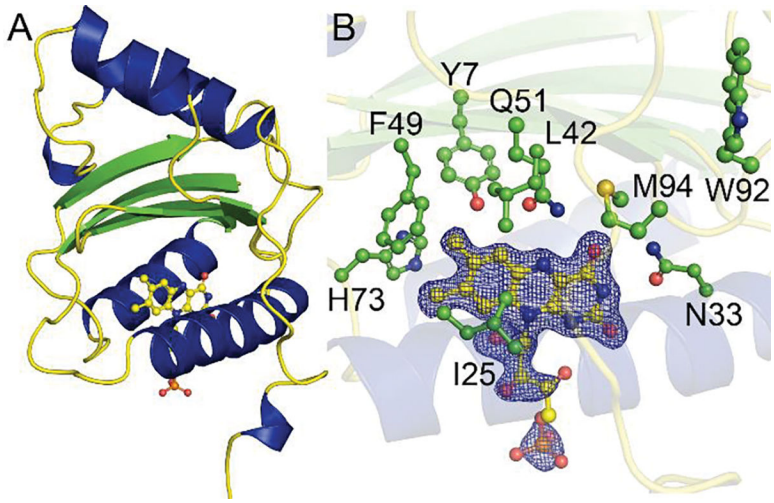

Figure 5. X-ray crystal structure of *A. baumannii* BlsA.

The *A. baumannii* BLUF protein, BlsA, has the characteristic ferredoxin fold with the chromophore sandwiched between the N-terminal pair of helices (A, α-helices colored blue, β-strands colored green, and loops colored yellow; the flavin chromophore is shown in ball-and-stick representation with yellow carbon atoms, blue nitrogen atoms, red oxygen atoms and orange phosphate atom). A closer examination of the flavin binding pocket (B) shows the conserved residues that interact with the chromophore and are implicated in the photoactivation mechanism. The side chains are shown in ball-and-stick representation with green carbon atoms, blue nitrogen atoms, red oxygen atoms and yellow sulfur atom. The chromophore is represented as in (A) and is shown modeled into the $F_{obs} - F_{calc}$ map, contoured at 3 σ, that was generated prior to addition of the ligand.

Author Manuscript Author Manuscript Author Manuscript Author Manuscript

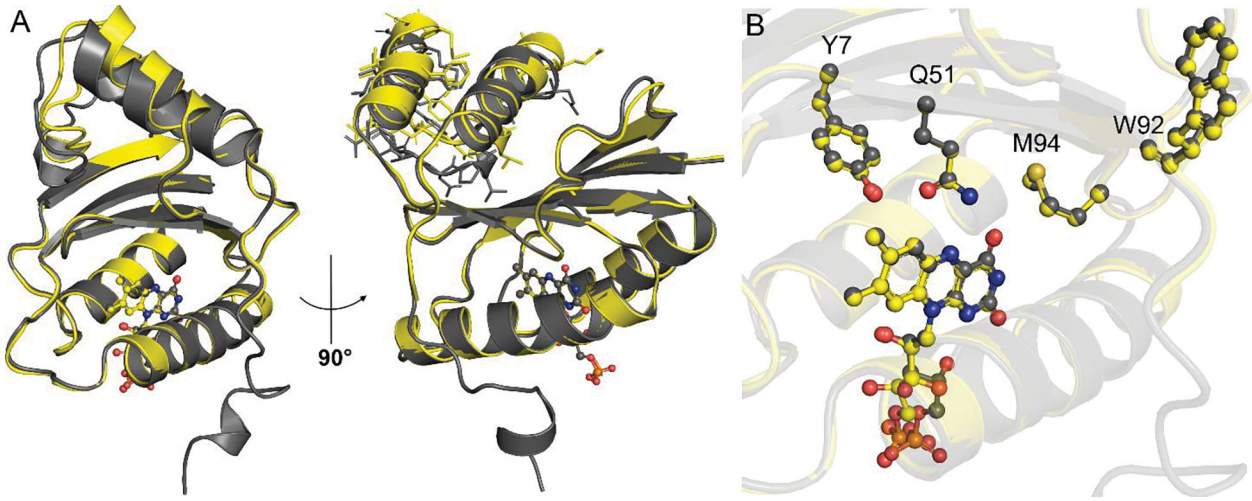

Figure 6. Comparison of BlsA ground state and photo-activated state structures.

Upon photoactivation with blue light (455 nm), BlsA undergoes significant structural changes. Superposition of the photoactivated structure (yellow) with the ground state structure (gray) reveals a large conformational change of the two helices making up the variable domain (A). The side chains on these helices translate between 1 and 6 Å from dark to light state. In addition, the C-terminal 11 resides become unstructured upon photoactivation. Despite the large structural rearrangements of the protein, very little change is observed in the flavin binding pocket (B).

Author Manuscript Author Manuscript Author Manuscript Author Manuscript

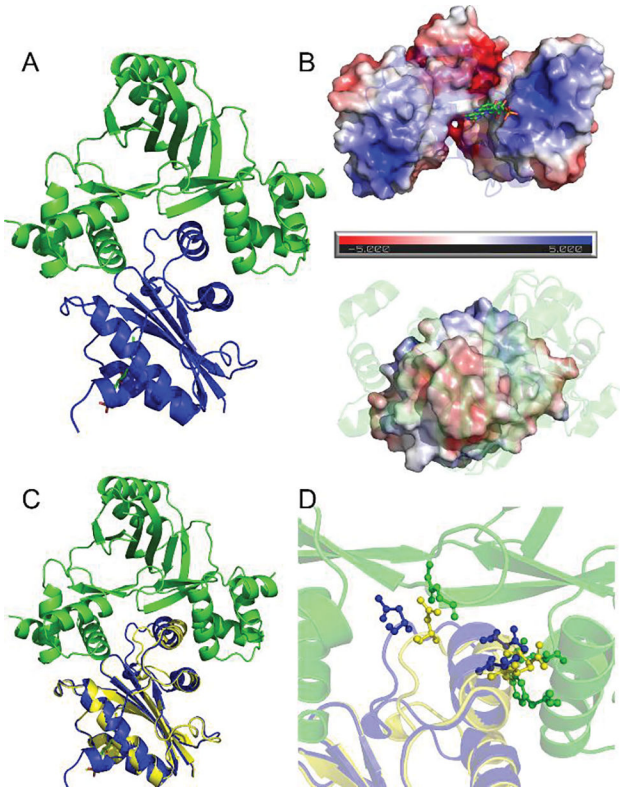

Figure 7. Putative model for BlsA interaction with Fur.

Protein-protein docking experiments, using the ZDOCK server, revealed a potential binding interaction between ground state BlsA and Fur where the variable domain of BlsA occupies the Fur DNA-binding site (A). Analysis of the surface charge distribution of Fur (B, top, green) and BlsA (B, bottom, blue) shows that the variable domain of BlsA is electronegative (B, lower half, pink region), while the lobes of FUR are highly electropositive (B, top half, blue region). The predominantly electronegative surface of the variable domain would make favorable contacts with the basic surface in the DNA binding groove of Fur. Superposition of the photo-activated state structure of BlsA (C, yellow) to the docked ground state of BlsA (C, blue) reveals a number of sidechain and mainchain clashes (D) that would occur between BlsA and Fur upon BlsA photoactivation.

Author Manuscript Author Manuscript Author Manuscript Author Manuscript

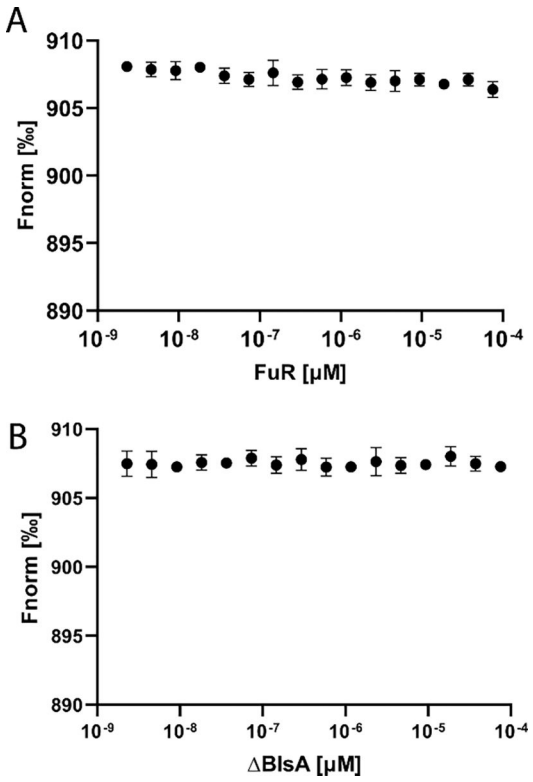

Figure 8. Interaction between $BlsA_{del101–110}$ and FUR.

Microscale thermophoresis was used to measure the affinity of BlsA lacking a helix in the variable domain ($BlsA_{del101–110}$) and Fur. The MST data shows very little or no interaction between $BlsA_{del101–110}$ and Fur (A), similar to what is observed in the negative control (B, BlsA and BSA).

Author Manuscript Author Manuscript Author Manuscript Author Manuscript

Table 1:

Data collection and refinement statistics

	BlsA – ground state	BlsA – photoactivated
Data Collection:		
PDB ID	6W6Z	6W72
Beamline	AMX 17-ID-1	AMX 17-ID-1
Detector	Eiger 9M	Eiger 9M
Wavelength (Å)	0.9792	0.91979
Resolution range (Å)	47.2 – 1.71	29.63 – 1.76
Space group	*C*2	$P2_1$
Unit cell dimensions		
a,b,c (Å)	92.87, 37.44, 49.27	48.40, 39.29, 92.82
β (°)	106.57	103.80
No. of measured reflections	91,579	134,010
No. of unique reflections	17,106	32,248
Mean I/sigma(I)	31.6 (1.07)	10.8 (1.5)
Completeness (%)	96.5 (61.7)	94.6 (57.3)
Redundancy	5.2 (2.1)	4.2 (3.2)
R_{merge} (%)	0.09 (0.70)	0.07 (0.64)
$CC_{1/2}$	0.997 (0.509)	0.998 (0.854)
Data Refinement		
Total no. of reflections	16,259	30,701
Test set	846	1,542
$R_{work}/R_{free\ (\%)}$	0.185 / 0.222	0.192 / 0.237
No. of protein atoms	1,221	2,348
No. of ligand atoms	31	62
No. of water atoms	95	266
R.M.S.D.		
bonds (Å)	0.01	0.01
angles (deg)	1.7	1.7
Mean B factor ($Å^2$)	24.6	23.3
Ramachandran plot (%)		
Favored	96.1	97.8
Outliers	0	0
MolProbity Clashscore (%)	6.17 (91)	4.44 (97)